

Review

A Review of Torque Ripple Reduction Design Methods for Radial Flux PM Motors

Sergio I. Suriano-Sánchez, Mario Ponce-Silva *, Víctor H. Olivares-Peregrino and Susana E. De León-Aldaco 

Tecnológico Nacional de México, CENIDET, Cuernavaca P.C. 62490, Morelos, Mexico

* Correspondence: mario.ps@cenidet.tecnm.mx

Abstract: Nowadays the efficient use of energy is a major issue in applications such as electric vehicles. However, there are some phenomena that affect electric vehicle performance. One of those phenomena is the torque ripple of electric motors, which interferes with traction and the suspension system (causing vibration that stresses this system), and it can also introduce electric current harmonics into the battery, reducing its life, since torque ripple is partly a consequence of non-sinusoidal back EMF. For those reasons this is a topic worth investigating. The torque ripple of permanent magnets (PM) motors can be reduced in design or through control. Since control techniques have been reviewed and design methods have not, this paper presents a comparison of several design techniques to reduce torque ripple by different approaches and categorize them to show the characteristics of each group. A discussion is then made about the advantages and disadvantages of the designs, in general, as well as some comments about the missing, but important information, in the papers, such as the effects on efficiency. The study shows that a combination of methods provide the best results, although it complicates fabrication and suggests that this is a promising line of future investigation on torque ripple reduction methods.

Keywords: torque ripple; cogging torque; air-gap flux density; back EMF; geometry optimization



Citation: Suriano-Sánchez, S.I.; Ponce-Silva, M.; Olivares-Peregrino, V.H.; De León-Aldaco, S.E. A Review of Torque Ripple Reduction Design Methods for Radial Flux PM Motors. *Eng* **2022**, *3*, 646–661. <https://doi.org/10.3390/eng3040044>

Academic Editors: Antonio Gil Bravo and Gilmar Ferreira Batalha

Received: 24 October 2022

Accepted: 6 December 2022

Published: 9 December 2022

Publisher's Note: MDPI stays neutral with regard to jurisdictional claims in published maps and institutional affiliations.



Copyright: © 2022 by the authors. Licensee MDPI, Basel, Switzerland. This article is an open access article distributed under the terms and conditions of the Creative Commons Attribution (CC BY) license (<https://creativecommons.org/licenses/by/4.0/>).

1. Introduction

Torque ripple is one of the undesired, but inherent, properties in motors with permanent magnets. The main causes of torque ripple are non-ideal back EMF waveforms, saturation of the machine's magnetic circuit, and cogging torque [1]. Cogging torque appears because of the attraction between rotor's permanent magnets and stator teeth, since they are made with ferromagnetic materials. When the magnet aligns with the maximum amount of stator teeth, the reluctance seen by the magnet flux is minimized, but increases as the rotor turns and the magnets move [2]. The increase of reluctance produces a force that tries to return the magnet back to alignment, and as a result, the instantaneous torque varies periodically in time [2]. This effect is especially important at low speed; at higher speed, inertia helps to minimize the drawbacks of cogging torque because the tendency of the rotor to move becomes considerably stronger than the attraction between the magnets and stator teeth, so that the effects of cogging torque in the motor's performance are decreased, although the cogging is still present.

The saturation of machine's magnetic circuit is a less common source of torque ripple, since it is almost always avoided in designs because of the additional problems that it brings. Saturation may increase torque fluctuations because not all the magnetic flux can pass through the path it should, so it has to move further in the airgap to find a way back to the magnet. In that process, the airgap flux density distribution is affected, and since airgap flux density is directly related to torque, higher fluctuations appear. In the literature revision, only one of the reviewed articles (the first cited one) mentions the saturation of machine's magnetic circuit, and its solution is briefly explained. However, it is important to take account of every possible cause of torque ripple to design better solutions.

In contrast, non-ideal back EMF waveforms are an important cause of torque ripple. Due to the magnet flux crossing the air gap, a voltage is induced in stator coils, and because of the rotor and stator geometric variables, the waveform of the induced voltage is usually not sinusoidal. This means that the back EMF has harmonics that interfere with the torque production. For its nature, this source of torque ripple is very hard to eliminate without affecting the machine's performance, especially the output torque, but it can be decreased to acceptable levels while keeping the machine's design parameters near to ideal.

In recent research on the innovations and design methodologies of permanent magnets motors, it was found that cogging torque and torque ripple reduction are topics that have been frequently investigated. Papers such as [3,4] show the relevance of better motor designs and the advances in this field, respectively, while [5] considers the effect of torque ripple in the suspension system of electric vehicles and [6] considers the consequences of motor's non-sinusoidal back EMF on electric vehicle battery performance. However, control techniques for reducing torque ripple are more commonly reviewed and compared than design methods, although there are a wide range of innovations in this field.

Control methods are preferred when the machine is already designed and optimized, and trying to reduce torque ripple by modifying the geometry could affect the desired performance. Additionally, design methods may complicate the manufacturing process and, hence, increase costs. The operating principle in the control methods is commonly the injection of current harmonics on top of the operating currents. This can be made by current reference-based methods, parameter-based methods, and adaptive methods [7].

Nonetheless, reducing torque ripple through control requires extra circuitry, which leads to higher risk of failure and more need of maintenance, and it also requires specialized personnel. When designing a motor, the requirements of the application should be considered, so that the best torque ripple reduction method is used, be it through design or control.

Since control techniques have been more broadly reviewed, such as, for instance, in [7–11], the objective of this paper is to provide information about the different design methods for torque ripple reduction in several topologies of permanent magnets motors. For that purpose, the design methods are classified in three groups, which are: geometry optimization, slot/pole number combination, and stator winding type. In every category, some application examples from research papers are presented, and readers are encouraged to refer to those papers for mathematical and experimental details.

The paper is structured as follows: Section 2 is a review of torque ripple reduction design techniques, following the above-mentioned classification, as well as how they work. In this section, a comparative table with relevant information, found in the literature, is presented, and some of the most common and interesting methods are described, based on papers where such methods are applied. Section 3 is a discussion of the information and the data reviewed, where the advantages and disadvantages of every category from Section 2 are mentioned, as well as the missing, but important, information in the papers and the future research that could be useful for designers. Finally, conclusions summarize the information found in the literature and the results of its analysis, as well as the possible future works.

2. Torque Ripple Reduction Design Methods

There are several options for reducing torque ripple, depending on the cause of it, such as geometry optimization, specific slot/pole combinations, or stator winding type. Once the source of ripple is found and understood, the optimal method or combination of methods to reduce it should be applied. This section reviews various design methods to reduce the torque ripple of rotor PM machines by different approaches, and Table 1 summarizes some relevant information about them, including a couple for stator PM machines.

Table 1. Relevant data of the revised torque ripple reduction design techniques.

Reference	Machine Topology	Design Technique	Torque Ripple Reduction Ratio (%)	Slot/Pole Number	Rated Power (W)	Average Torque (Nm)	Rated Speed (rpm)
High Torque Density and Low Torque Ripple-Shaped Magnet Machines Using Sinusoidal Plus Third Harmonic-Shaped Magnets [12]	Radial flux, surface permanent magnets	Magnets shaping	88.50	24/8	54	184	2800
A Dual Notched Design of Radial-Flux Permanent Magnet Motors with Low Cogging Torque and Rare Earth Material [13]	Radial flux, surface permanent magnets	Gear-shaping the surfaces of magnets and teeth	62.8	18/12	80	–	10,000
Torque Ripple Reduction of Saliency-Based Sensorless Drive Concentrated Winding IPMSM Using Novel Flux Barrier [14]	Saliency-based, interior permanent magnets	Flux barrier design	28	9/6	5500	45	1750
Reduction of Torque Ripple in Consequent Pole Permanent Magnet Machines Using Staggered Rotor [15]	Consequent-Pole permanent magnet motor	Staggered rotor design	60	9/6	–	2.13	1500
Optimal Design to Reduce Torque Ripple of IPM Motor with Radial-Based Function Meta-Model Considering Design Sensitivity Analysis [16]	Radial flux, interior permanent magnets	Slots, teeth, and magnet size optimization	58	48/8	50,000	400	1200
Permanent Magnet Motor Design for Satellite Attitude Control With High Torque Density and Low Torque Ripple [17]	Radial flux, dual rotor	Slotless windings and Halbach array magnets	67	9/8	11.5	32.15 m	6000
Optimization of Torque Ripples in an Interior Permanent Magnet Synchronous Motor Based on the Orthogonal Experimental Method and MIGA and RBF Neural Networks [18]	Radial flux, interior permanent magnets	Stator, rotor, and magnets sizes optimization	84	24/8	5010	4.2	–
Asymmetric Rotor Design of IPMSM for Vibration Reduction Under Certain Load Condition [19]	Radial flux, interior permanent magnets	Asymmetric rotor shape	33.10	12/8	5000	24	2000
Ferrite PM Optimization of SPM BLDC Motor for Oil-Pump Applications, According to Magnetization Direction [20]	Brushless DC	Parallel magnetization direction of permanent magnets	69.20	12/8	126	0.33	3200
Design and Analysis of Halbach Ironless Flywheel BLDC Motor/Generators [21]	Brushless DC, outer rotor	Halbach array magnets	20	6/8	–	800 m	40,000
Design Optimisation of an Outer Rotor Permanent Magnet Synchronous Hub Motor for a Low-Speed Campus Patrol EV [22]	Radial flux, outer rotor	Similar number of slots and poles	29	51/50	–	94.5	600
Effect Comparison of Zigzag Skew PM Pole and Straight Skew Slot for Vibration Mitigation of PM Brush DC Motors [23]	Brush DC	Zigzag skewed magnets	37.5	24/4	800	2.147	2700
Analytical Prediction and Optimization of Cogging Torque in Surface-Mounted Permanent Magnet Machines With Modified Particle Swarm Optimization [24]	Radial flux, surface permanent magnets	Air-gap length and magnet thickness optimization, fractional slot-pole number, and parallel magnetization of permanent magnets	92.48	12/8	–	–	–
Material-Efficient Permanent Magnet Shape for Torque Pulsation Minimization in SPM Motors for Automotive Applications [25]	Radial flux, surface permanent magnets	Magnets shaping and skewing	86.1	6/4	264.4	0.5053	1000
Modeling of Novel Permanent Magnet Pole Shape SPM Motor for Reducing Torque Pulsation [26]	Radial flux, surface permanent magnets	Magnets shaping	72.08	6/4	340.48	0.6503	5000
Reduction of Torque Ripple Caused by Slot Harmonics in FSCW Spoke-Type FPM Motors by Assisted Poles [27]	Spoke-type	Fractional slot concentrated winding and assisted poles	40	12/10	–	6.5	1500

Table 1. Cont.

Reference	Machine Topology	Design Technique	Torque Ripple Reduction Ratio (%)	Slot/Pole Number	Rated Power (W)	Average Torque (Nm)	Rated Speed (rpm)
Torque Ripple Reduction in Five-Phase IPM Motors by Lowering Interactional MMF [28]	Radial flux, interior permanent magnets	Asymmetrical rotor poles shifting	–	40/8	–	10.45	1500
Torque Ripple Reduction of a Salient Pole Permanent Magnet Synchronous Machine, with an Advanced Step-Skewed Rotor Design [29]	Salient-pole, surface permanent magnets	Eccentric airgap, advanced step-skewed rotor, and pole shoes skewing	91	36/4	1500	10.52	1500
Efficient Utilization of Rare Earth Permanent-Magnet Materials and Torque Ripple Reduction in Interior Permanent-Magnet Machines [30]	Radial flux, interior permanent magnets	Rotor made by segments arranged in the axial direction, and pole shaping	50	48/8	68,000	210	3080
Investigation of Short Permanent Magnet and Stator Flux Bridge Effects on Cogging Torque Mitigation in FSPM Machines [31]	Flux-switching	Short magnet and stator flux bridge	32.70	12/10	500	3.05	1500
Reduction of Torque Ripple in Inset Permanent Magnet Synchronous Motor by Magnets Shifting [32]	Radial flux, interior permanent magnets	Magnets shifting	28	48/8	–	244	–

– Not reported.

2.1. General Classification

Figure 1 shows the general torque ripple reduction approaches reviewed and the different design methods in each of them. It is visible that geometry optimization is the widest category, followed by stator winding type and slot/pole number combinations.

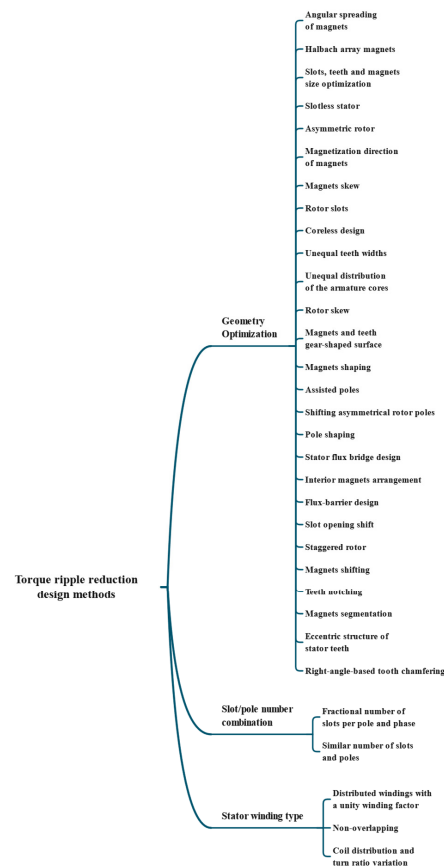


Figure 1. General classification of torque ripple reduction design methods.

2.2. Slot/Pole Number Combination

Since cogging torque is one of the main torque ripple components, it is important to find ways to reduce it. Fortunately, there is a relatively easy way to minimize cogging torque, which is designing the machine with a specific combination of slots and poles. However, this category of methods to reduce torque ripple is the one with the smallest number of design variations found in the research. One possible reason for this lack of diversity could be that the existing methods for finding the optimal slot/pole number are good enough to minimize cogging torque in most cases. Sections 2.2.1 and 2.2.2 introduce examples of this torque ripple reduction category.

2.2.1. Fractional Slot/Pole Number Design

The fractional slot/pole number reduces the cogging torque because the magnets align differently with the stator teeth, producing cogging torques in opposite directions, which tend to cancel each other out. When the right combination of slots and poles is selected, a substantial reduction in cogging torque is possible. Some reviewed articles dealt with cogging torque and tried to eliminate it or reduce it by experimenting with different slot/pole number combinations [22,24,33–44]. One of those articles is [33], which showed the advantages of machines with fractional number of slots per pole and phase, not only in generating less cogging torque and torque ripple, but also having acceptable values of electromagnetic torque and copper losses, compared with machines with integer number of slots per pole and phase.

In the paper, two motors with equal dimensions, but different slot/pole number, were tested. One motor was designed with 18 slots and 20 poles (fractional slot/pole number), while the other had 60 slots and 20 poles (integer slot/pole number). One thing to consider is that there is no explanation in the paper of why they selected those specific numbers. The presented results showed that total torque waveform is much smoother in the fractional slot/pole number machine than in the integer slot/pole number motor. That is because cogging torque values are significantly lower, as is also shown in the paper. In addition, the average torque results were highly similar, as well as the power output and losses. It is important to consider that all results were obtained from simulation and not from experimental tests, so there may be differences in practice. The only drawback of fractional slot/pole number motors seems to be that design is more complicated, since a number of slots per pole and phase different than 1 lead to the necessity of distribution factors for the back EMF estimation, and those factors are usually inaccurate.

2.2.2. Similar Number of Slots and Poles Design

Another article related to the cogging torque reduction using fractional slot/pole numbers is [22], where the approach is to use a similar number of slots and poles, which seems to be a popular technique in the study of direct drive motors. In that specific case, the number of poles is the number of slots minus one. According to the findings in that paper, motors with similar number of slots and poles have better features than traditional integer slot and poles motors, such as high efficiency, high power density, short winding ends, low torque ripple, and better weakening capability [22]. In addition, three designs with 27/26, 51/50, and 75/74 slot/poles were simulated. The one with the best results for the required application was the 51 slots and 50 poles design. The reason for the cogging torque reduction is that there is no common divisor of 51 and 50, which can reduce the slot effect successfully because it leads to an alignment of the magnets with the stator teeth that produce opposite cogging torques, which cancel each other out almost completely at any rotor position, as is explained by the author in [22].

However, selecting a similar number of slots and poles is not enough to solve the torque ripple problem and to obtain all the mentioned benefits. That is because the slot number may lead to the need of specific winding arrangement, which affects copper losses and back EMF harmonic content. The optimal number of slots, poles, and winding

approach must be determined for each design by following the methodology described in the paper, which includes FEA analysis.

2.3. Stator Winding Type

Back EMF harmonics are the other main cause of torque ripple in permanent magnet machines. This issue can be addressed by two approaches: using a specific stator winding type, modifying rotor, and/or stator geometry. In this section, three winding approaches to minimize back EMF harmonics are presented, and papers that dealt with this method to reduce torque ripple are used as examples.

2.3.1. Use of Distributed Winding

To prevent undesired back EMF harmonics, winding methods have been developed and tested in [22,34,44–53]. For example, ref. [34] gives a study between concentrated versus distributed windings. There, the advantages of both winding types are presented, and the author remarks that concentrated winding can generate sub-harmonic MMF components. In the results section, it was found that cogging torque in concentrated winding designs was much larger than the distributed ones, in which the cogging torque is very close to zero [34]. Still, the on-load torque ripple results were just slightly lower because of the interaction between stator and rotor magnetic fields, which create a non-uniform airgap flux density and flux linkage; therefore, non-sinusoidal back EMF was produced.

Another disadvantage of the concentrated winding is that it produces high noise and vibration, due to radial forces generated from the interaction between the permanent magnet airgap field and the stator MMF field [34], which also contributes to the increase in torque ripple.

The results in the cited paper show a comparison of the harmonic content found in the three designs tested. The 12-slot design corresponds to the one with concentrated winding, while 33 and 36 slot use distributed winding. Although 33-slot motor has the largest 3rd harmonic, the author explains that it is suppressed by the winding star connection and, therefore, has no impact on performance [34]. With that said, it is clear that this design is better when it comes to back EMF harmonics reduction, which helps to decrease the total torque ripple. That is because distributed winding creates a more uniform current and magnetic field distribution around the rotor.

Because of its characteristics, distributed winding designs seem to be better choices for electrical vehicle applications. However, when the machines are thermally constrained, concentrated winding design manages higher power, although distributed winding gives better heat transfer in the slots, which helps reducing additional copper and iron losses.

2.3.2. Use of Non-Overlapping Windings

A second technique aimed to reduce torque ripple by winding modification is the use of non-overlapping windings, as shown in [45], where a study on the characteristics of overlapping and non-overlapping windings is presented, and both winding types are applied in modular dual three-phase permanent magnet machines.

In the study, a 42-slots/32-poles motor with non-overlapping winding is compared with a 192-slots/32-poles motor with overlapping winding. Based on performance results, the author states that non-overlapping winding design has similar average torque and efficiency, compared to overlapping winding design. In addition, the non-overlapping winding design presents much lower torque ripple, regardless of the current value, as well as shorter and simpler end windings [45]. The torque ripple reduction in the dual three-phase non-overlapping fractional slot winding machine occurs because this kind of machine inherently has twelve semi-phases, and a higher number of phases leads to less current harmonics. Besides, due to smaller mutual inductances between phases and larger d-axis inductance, the non-overlapping winding design tends to be more fault tolerant [45].

The back EMF waveforms of both designs are similar, but non-overlapping winding design has lower magnitude harmonics. Cogging torque is significantly lower, as well.

Even under load conditions, torque ripple of non-overlapping winding machine is much smaller than that of overlapping winding machine. That is because the armature field is much weaker than the permanent magnets field, so airgap flux density distribution is not highly affected unless the current is increased, which would create a stronger armature field. However, experimental results showed slightly higher torque ripple than expected, and the author's explanation for that was manufacturing errors, so fabrication complexity of this kind of motor should be considered.

2.3.3. Coil Distribution and Turn Ratio Variation

Another method intended to minimize torque ripple, this time by electromagnetic force (EMF) voltage distortion reduction, is varying coil distribution and turn ratio. An example of this is [48]. In that paper, triple layer and quadruple layer windings with varied coil turns were tested and compared with conventional single layer and double layer machines. It was found that the proposed designs can reduce torque ripple and greatly enhance the flux weakening capability. Of course, the coil turn ratios must be optimized to reduce the voltage distortion ratio. It is important to keep the number of turns in series per phase identical to that of the double layer and single layer during turn ratio optimization, so that $2N_1 + 4N_2 = 4N_{Dual\ Layer} = 2N_{Single\ Layer}$ for the triple layer motor and $4N_1 + 4N_2 = 4N_{Dual\ Layer} = 2N_{Single\ Layer}$ for the quadruple layer motor.

The reason that triple layer winding with optimal turn ratios reduces voltage distortion is that the armature leakage flux and permanent magnets leakage flux in the tooth tips will not reverse polarities at the same time, so instead of summing, the tooth tip leakage fluxes tend to cancel each other out, thus smoothing the airgap flux density distribution and reducing the phase voltage distortion. Quadruple layer winding works because the amplitude of armature tooth tips leakage flux is attenuated [48]; therefore, the total tooth tip leakage flux, decreases which has a similar effect to that of triple layer winding.

From the tests made in the cited paper, it is clear that triple layer winding has the lowest ripple, while keeping almost the same average torque. That is to be expected, since the triple layer winding machine reduces the tooth tip leakage flux almost completely by the before explained mechanism, while the quadruple layer winding machine only minimizes the armature tooth tip leakage flux, but keeps permanent magnet tooth tip leakage flux unchanged. However, this design approach has the disadvantage of a complex manufacturing process, due to the necessity of combining multiple and different coils, and motor radius may need to be increased, so the slots have enough space for all the winding layers.

2.4. Geometry Optimization

As shown in Figure 1, there are plenty of possible approaches to reduce torque ripple by geometry optimization [1,12–21,23–32,35,38,40,43,44,46,47,52–96]. However, all those approaches aim to reduce torque ripple by minimizing cogging torque or back EMF-related issues. The rest of this section will present some of the most interesting geometry optimization methods found in the literature and a brief explanation of them.

2.4.1. Asymmetric Rotor Design

One popular geometry optimization method to reduce torque ripple in IPM motors under the desired load condition is the use of an asymmetric rotor. This method is intended to modify the airgap flux density distribution to make it sinusoidal, therefore eliminating back EMF harmonics and minimizing torque ripple. Due to the placement of the magnets, the airgap flux density is higher near the magnets and lower between them, but the transition is not regular in non-shaped rotors, which leads to non-sinusoidal airgap flux density distribution. Therefore, an asymmetry is implemented in the rotor iron between the magnets to modify the airgap length in a way that the airgap flux density distribution becomes sinusoidal.

Using a numerical formula known as the advanced inverse cosine function (AICF), in [19], the design of an asymmetric rotor for an 8-pole, 12-slot 5 kW spoke type interior permanent magnet motor was developed. The AICF is an equation that gives the needed airgap length to make airgap flux density sinusoidal. It comes from the analysis of the interaction between the airgap magnetomotive force by the magnets and the airgap magnetomotive force by the armature reaction. After all the analytic process, the AICF is expressed as $l_g(\theta) = \frac{l_d}{\sin \theta} - k_F \frac{l_d \sin(\theta + \beta)}{\cos \theta}$, where $l_g(\theta)$ is the airgap length as a function of the electrical angle, θ , l_d is the d-axis the airgap length, k_F is the magnetomotive force ratio, and β is the current phase angle [19].

The optimized geometry of the rotor with this method makes the air-gap flux density sinusoidal under the desired load condition, which reduces radial electromagnetic forces, and hence, minimizes torque ripple to some extent [19].

One drawback of this design method is that the final rotor shape fulfils its goal of minimize torque ripple only for the designed load condition, so the kind of motor is not suitable for varying load applications. Additionally, fabrication is complex.

2.4.2. Special Permanent Magnets Magnetization Direction

One particular way to minimize torque ripple that does not affect machine's shape is optimizing the permanent magnets magnetization direction. For example, ref. [20] achieved maximization of back EMF and torque density, while reducing the torque ripple. Then, radial and parallel magnetization were compared using ferrite and neodymium magnets in a brushless DC motor. The objective of these tests was to develop high performance and low torque ripple motors using ferrite magnets, instead of rare-earth ones, to reduce costs. Additionally, the author stated that, in surface permanent magnet brushless DC motors, radial magnetization is commonly used to obtain squared back EMF and reduce torque ripple, but this is only true for neodymium magnets and not for ferrite magnets.

Four motors were compared: two neodymium magnets motors and two ferrite magnets motors with radial and parallel magnetization for both cases. At no load, parallel magnetization motors showed higher airgap flux density than radial magnetization motors, and both ferrite magnet motors produced sinusoidal back EMF waveforms, while only the radial magnetization neodymium magnets motor produced a rectangular back EMF waveform. On load operation, at 3200 rpm, all models exhibited almost the same average torque, but parallel magnetization ferrite magnets motor presented the lowest torque ripple of 16.3%.

Although parallel magnetization ferrite magnets motor had good performance, one disadvantage of ferrite magnets machines is that airgap flux density is very low, so stator teeth dimensions need to be minimized and maximize the coil copper area to increase electric loading. However, small tooth tips lead to higher undesired leakage flux.

The general results show that parallel magnetization is better, since it concentrates the flux line, thus increasing the air-gap magnetic field density, which increases the magnetic loading [20]. Additionally, with this magnetization the phase current at rated power decreases, improving the motor efficiency.

2.4.3. Magnet Skewing

Magnet skewing is another method to reduce torque ripple and vibration with the advantage of not requiring modifications in the motor structure, which reduces manufacturing costs and simplifies production process. Additionally, different skew approaches have been developed. One of them was presented in [23], where a zigzag skew was tested and compared with straight-skewed slot to minimize the vibration in a permanent magnet brush DC motor.

The straight-skewed slot has an effect on torque ripple and vibration because different segments of conductors are placed on different positions of the harmonic magnetic field; therefore, the EMF phases of different conductor segments are different, and since the total conductor EMF is the sum of individual conductor segments EMF, choosing the right skew

angle leads to harmonics cancelation, while the fundamental component of magnetic field is almost not affected. Additionally, slot skew helps minimize cogging torque by making the difference of reluctances as small as possible for different rotor positions. Hence, the goal of this skew type is to mitigate tooth harmonic EMF and cogging torque.

However, the straight-skewed slot does not reduce vibration as it does for cogging torque. The explanation given in the cited paper is that radial magnetic force distributes on the inner surface of magnets, and the resulting vibration is not the same in different points of the machine, so the forces cannot be added up directly to predict the vibration response. To solve this problem, zigzag skewed magnets, instead of straight-skewed slots, are proposed, which not only reduces vibration and torque ripple, but also simplifies manufacturing process. Zigzag skewed magnets create a regular radial magnetic force along the machine's axial direction, which minimizes vibration while keeping the mentioned advantages of straight-skewed slots.

One of the most relevant findings is that the permanent magnet pole is an elastomer and not an ideal rigid body [23], so this needs to be taken into account for electromagnetic analysis and vibration mitigation.

2.4.4. Unequal Teeth Widths Design

Now, changing to stator modification methods, using unequal teeth widths, such as in [58], is an interesting option to minimize back EMF-related sources of torque ripple. The type of motor discussed in the cited paper is fractional-slot, non-overlapping windings permanent magnet machine, also known as a tooth-coil winding permanent magnet synchronous machine (TCW PMSM). In this specific motor type, adjacent teeth may have different flux densities, due to the interaction between magnets and armature fluxes at the loaded conditions. That happens due to different synchronous inductance values, which create different armature reactions.

According to the issues mentioned before, designing TCW PMSMs with equal tooth widths may lead to different iron permeabilities or even saturation, therefore producing torque ripple. To solve this problem, the right width for each tooth must be found, so that all teeth have approximately the same flux density. One important detail to consider is that, in the optimum teeth widths design, compared to an equal teeth widths motor, the width of one stator tooth was increased the same amount that the adjacent tooth was decreased, so the total iron used in stator remains the same.

With this method, the reduction of the lowest orders torque ripple harmonics (6th and 12th in the cited paper) is achieved. In addition, surface mounted PM and interior PM designed with this approach were studied, as well as the effect of PM skewing in torque ripple reduction, and the results were satisfactory. However, the disadvantage of this method is that it gives the desirable results for only one working point [58]. Additionally, when the number of slots increase and more than two teeth widths need to be adjusted, adjacent slot areas become different, and the stator has to be modified to keep the slot areas the same, and of course, stator fabrication becomes more complicated and expensive.

2.4.5. Stator Teeth and Magnets Surfaces Notching

Notching is a different geometry optimization method to mitigate torque ripple. Usually, teeth's surfaces are notched, aiming to reduce cogging torque. The case presented in [13] combines teeth and magnets notching not only to obtain better output torque characteristics, but also to reduce the quantity of material needed for rare earth magnets and hence reducing costs. The paper proposes gear-shaped structures for the permanent magnets and stator teeth of four models with different mechanical angles and depths.

The cogging torque reduction obtained by teeth and magnets notching occurs because the notches modify reluctance forces making them almost equal in all directions, no matter the position of the rotor; therefore, similar cogging torques appear in opposite directions, and they cancel each other. To some extent, the effect is similar to that of using fractional slot/pole number, with the salient parts of teeth and magnets acting like small slots and

magnet poles, with the advantage of being able to design the motor with any slot/pole number.

In the cited paper, four models of notched magnets and teeth were proposed, each with different depths and number of notches. Since no theoretical analysis was conducted, all models were compared by finite element analysis simulations. First, the notched magnets were individually simulated with non-notched teeth, and notched teeth were simulated with regular magnets. Then, all possible combinations of notched magnets and teeth were simulated to find out the better combination to mitigate cogging torque, while keeping the average torque reduction to its minimum.

After the tests, the model combination with the best results was the PM-1 (magnets with notches of 0.3 mm depth and 3 degrees of angular space between notches) and ST-2 (teeth with notches of 0.3 mm depth and 2.5 degrees of angular space between notches), which achieved 62.8% cogging torque reduction, 6.7% less rare earth material needed, and only 6.5% average torque reduction, compared with a non-notched design. The disadvantages of this torque ripple reduction method are stator fabrication complexity and average torque reduction, due to magnet material decrease.

2.4.6. Magnets Shaping

Another method based on motor's permanent magnets modification is magnet shaping. For this case, ref. [12] is used as example. The principle here is to shape the permanent magnets on the axial direction, according to back EMF's fundamental plus third harmonic. As was mathematically demonstrated in the cited paper, the induced back EMF waveforms follows exactly the shape of magnet's cross-sectional area, thus shaping the magnets according to a sinusoid plus a third harmonic produces a rotor magnetic loading that contains only those components and hence torque is produced only by the fundamental components of electric and magnetic loadings [12]. The third harmonic enhances the fundamental component, which improves torque density, while torque ripple is almost zero because of the absence of other harmonics.

The complete designed magnets consist of two identically shaped magnets placed "back-to-back", which minimizes the unbalanced axial force, and the magnet's thickness is constant, so the demagnetization force can be uniformly handled in the radial direction.

In addition to the sinusoid plus third harmonic-shaped magnet, a regular rectangular magnet and a pure sinusoid-shaped magnet were tested to compare their performances. Rectangular magnets produced the highest torque, for they use maximum possible quantity of magnet material, but the induced back EMF contained plenty of harmonics that cause torque ripple. Sinusoid plus third harmonic-shaped magnets produced slightly lower torque, with the advantage of eliminating torque ripple. Pure sinusoid-shaped magnets produced the lowest torque, since the quantity of magnetic material is the lowest, as well, but torque ripple was eliminated. All models showed uniform flux density distributions.

The results prove that the proposed design makes an efficient use of permanent magnet materials, and its torque density is similar to the one from regular rectangular magnets motor, while keeping torque ripple near zero. Additionally, the magnet's resistivity is not compromised against a demagnetization force because of constant radial width. The only drawback of this design approach is the manufacturing complexity of magnets.

2.4.7. Staggered Rotor Design

A particular design to reduce torque ripple by back EMF smoothing is the staggered rotor, as shown in [15]. In that study, a consequent pole permanent magnet (CPM) motor was designed and built using staggered rotor to eliminate the back EMF even-order harmonics and reduce cogging torque, thereby considerably decreasing the torque ripple [15]. However, staggered rotor presents considerable axial leakage flux, so an axial flux barrier (airgap between the rear and front parts of the rotor) was necessary to reduce it. Still, it was possible to take advantage of the flux barrier by embedding the magnets in it.

In conventional CPM machines, the flux passing through the magnet-poles and iron-poles is the same, but due to the difference of reluctance under one pole pair, the airgap flux density becomes asymmetric and contains even-order harmonics, which affect back EMF smoothness and cause torque ripples. In the proposed staggered rotor CPM machine (SCPM), there is an airgap between the rear and front parts, so the SCPM machine can be considered as two submachines, while the coils of both of them are considered in series connection because both submachines share the same armature winding. Therefore, the phase back EMF in SCPM machine can be approximated to the sum of both submachines back EMF. Since the staggered degree is 180 electrical degrees and magnets magnetization direction is opposite in both rotor parts, the sum of the phase back EMF induced by the rear and front rotor parts results in the elimination of even-order harmonics. Cogging torque is reduced by the same mechanism: the superposition of cogging torques produced by the rear and front parts of the rotor results in the elimination of the cogging torque odd-order harmonics.

One last modification was made in the designed motor. Since the airgap between the rear and front parts of the rotor reduced the effective rotor length, the SCPM machine had a lower fundamental back EMF than the regular CPM machine. To solve that problem, one axially magnetized magnet can be embedded in the rotor airgap to concentrate the fluxes in the iron-poles which improves the airgap flux density above the iron-poles and the produced torque, although it slightly increases the cogging torque.

The proposed design performance was compared with that of the conventional CPM motor. The results verified that the staggered rotor CPM machine achieved a similar torque and PM utilization ratio, but remarkably lower torque ripple, compared with the conventional one [15].

2.4.8. Eccentric Structure of Stator Teeth Design

One last torque ripple reduction method is the design of stator teeth with an eccentric structure. This method is applied in [70] to an external rotor permanent magnet synchronous motor. The eccentric structure of stator teeth means that the center line of one magnet does not match the center line of one tooth or that the arc center of the tooth tip and the arc center of the magnet are not the same. To simplify the analysis, in the cited paper, only the second type of eccentricity is used. The effect of this modification is a variable airgap between the magnets and stator teeth, which modifies the airgap flux density. Furthermore, the analysis made by the author proves that this type of eccentricity minimizes the even-order harmonics of the airgap flux density, which reduces the torque ripple. Additionally, the eccentric arc of teeth tips contributes to cogging torque mitigation, due to the resulting shape of the stator teeth.

To compare the effect of different eccentricity values, four designs were simulated. As shown in the paper, as the eccentricity grows, the total torque ripple decreases up to 83.9%, compared to zero eccentricity design. However, the thickness of the tooth tip decreases with the increase of eccentricity, which may cause saturation at the tooth tip and affect the machine's performance if excessive eccentricity is used. Besides, due to the shape of teeth tips leakage, flux rises by a small amount, although it has little effect on the torque production.

To sum up, the results show that the eccentric structure of stator teeth has no important influence on the performance of the motor, but reduces the torque ripple and cogging torque effectively [70]. However, efficiency should be considered when selecting the eccentricity because excessive eccentricity will cause saturation of the magnetic circuit at the edge of teeth [70]. As for other geometry modification methods to mitigate torque ripple, this approach complicates stator manufacturing, which increases the total cost of the machine.

3. Discussion

As has been exposed, many solutions to the problem of torque ripple have been developed. The proposals are not only numerous, but also diverse, since they use all the possible

means, such as modification of the windings or magnets, optimization of geometric parameters, and even structural changes for stator and rotor to mitigate the causes of torque ripple. However, even when most of the reviewed papers claimed to minimize torque variations without affecting the average torque or even optimizing the quantity of permanent magnet material used, only a few of them, which are [1,20,22,30,31,34,45,56,57,61,62,65,70], considered the efficiency of the machine at the end of the tests. This is a major issue nowadays, when an optimal energy usage is always desirable. So, as for the case of the average torque, the efficiency levels should always be compared, and the trade-off between torque ripple reduction and efficiency should be explained in these kinds of papers.

It is also important to mention that some investigations are not completely dedicated to the problem of torque ripple, but they present some methods to minimize it. The inconvenience in these cases is that, usually, the effectiveness of the applied technique is not clearly reported, so it is difficult to determine whether the impact was important or not; therefore, there is not enough information to say if the technique should be further investigated.

One thing that is surely worth investigating is the validity of all the reviewed methods in different motor topologies, since most of them are applied to only one type of motor. This is important because different torque ripple reduction design methods may have different results when applied to one or another motor topology, and hence, the best solution for the designer's desired application is not obvious.

Another finding worth mentioning is that torque ripple reduction design methods can be applied simultaneously. Slot/pole combinations, winding arrangements, and geometry optimizations were combined in several of the reviewed papers. As expected, the correct combination of methods leads to a greater reduction of torque variations, as shown in Table 1 for the case of [24,29]. On the other hand, this practice brings more complex structures that are difficult to manufacture and increases the costs specially for the cases of stator and rotor asymmetries. That is the main drawback that often makes control techniques more popular to solve the torque ripple problem.

Anyhow, design methods have proven to be greatly effective in minimizing torque ripple, while keeping all the other parameters near the same even efficiency in the papers that report it. This is relevant because one of the main advantages of control techniques is precise ability to not affect the performance. Moreover, since control techniques are widely based on the injection of current harmonics on top of the operating currents, they might increase copper losses and, as a consequence, reduce efficiency, which is not necessarily the case for all the torque ripple reduction design methods.

4. Conclusions

Torque ripple reduction by design has demonstrated to be very effective and able to maintain the machine's performance with almost no changes. This enables it to compete with control techniques when the requirements of the application are favourable.

This paper presented a review of design methods to reduce torque ripple in permanent magnets machines. The advantages and disadvantages of the design methods and control techniques to achieve this goal were commented. The main design approaches to mitigate torque ripple were briefly explained, as well as the causes of torque pulsations. First, a general classification of the design methods was presented, then each category was individually focused and some of the most relevant papers about them were commented, and finally, the found and the missing information in the papers were discussed.

There are many design approaches to reduce torque ripple, and the main categories are the geometry optimization, use of special stator winding types, and slot/pole number combinations. It was found that all these deal with the same sources of torque ripple, which are cogging torque, back EMF-related issues, and saturation of the magnetic circuit. The largest category is geometry optimization, but the best results are obtained when more than one approach is implemented, although this complicates the fabrication process and increases the fabrication costs.

For future investigations, the impact of torque ripple reduction techniques in efficiency should be well-documented to know the convenience of each of them for different applications. Additionally, the papers that deal with torque ripple reduction should present the degree of reduction achieved, so that designers have a better idea of what method works better for their purposes. In addition, research on the effectiveness of the same torque ripple reduction design methods for different PM motors topologies are important to validate their generality.

Author Contributions: Conceptualization, M.P.-S. and S.I.S.-S.; methodology, S.I.S.-S. and M.P.-S.; software, S.I.S.-S.; validation, V.H.O.-P. and S.E.D.L.-A.; formal analysis, M.P.-S. and S.I.S.-S.; investigation, M.P.-S. and S.I.S.-S. and V.H.O.-P.; resources, S.I.S.-S. and V.H.O.-P.; data curation, S.I.S.-S. and S.E.D.L.-A.; writing—original draft preparation, M.P.-S. and S.I.S.-S.; writing—review and editing, M.P.-S. and S.I.S.-S. and S.E.D.L.-A.; visualization, V.H.O.-P. and S.E.D.L.-A.; supervision, V.H.O.-P. and S.E.D.L.-A.; project administration, M.P.-S. and V.H.O.-P.; funding acquisition, S.E.D.L.-A. All authors have read and agreed to the published version of the manuscript.

Funding: This research received no external funding.

Data Availability Statement: Not applicable.

Acknowledgments: This work was supported by National Council of Science and Technology (CONACYT).

Conflicts of Interest: The authors declare no conflict of interest.

References

- Mahmoudi, A.; Rahim, N.A.; Ping, H.W. Axial-flux permanent-magnet motor design for electric vehicle direct drive using sizing equation and finite element analysis. *Prog. Electromagn. Res.* **2012**, *122*, 467–496. [\[CrossRef\]](#)
- Hanselman, D.C. *Brushless Permanent Magnet Motor Design*; The Writers' Collective: Cranston, RI, USA, 2003.
- Zhu, X.; Fan, D.; Xiang, Z.; Quan, L.; Hua, W.; Cheng, M. Systematic multi-level optimization design and dynamic control of less-rare-earth hybrid permanent magnet motor for all-climatic electric vehicles. *Appl. Energy* **2019**, *253*, 113549. [\[CrossRef\]](#)
- Feng, S.; Magee, C.L. Technological development of key domains in electric vehicles: Improvement rates, technology trajectories and key assignees. *Appl. Energy* **2020**, *260*, 114264. [\[CrossRef\]](#)
- Long, G.; Ding, F.; Zhang, N.; Zhang, J.; Qin, A. Regenerative active suspension system with residual energy for in-wheel motor driven electric vehicle. *Appl. Energy* **2020**, *260*, 114180. [\[CrossRef\]](#)
- Uddin, K.; Moore, A.D.; Barai, A.; Marco, J. The effects of high frequency current ripple on electric vehicle battery performance. *Appl. Energy* **2016**, *178*, 142–154. [\[CrossRef\]](#)
- Lopez, C.A.; Jensen, W.R.; Hayslett, S.; Foster, S.N.; Strangas, E.G. A Review of Control Methods for PMSM Torque Ripple Reduction. In Proceedings of the 2018 XIII International Conference on Electrical Machines (ICEM), Alexandroupoli, Greece, 3–6 September 2018; pp. 521–526.
- Bondre, V.S.; Thosar, A.G. Study of control techniques for torque ripple reduction in BLDC motor. In Proceedings of the 2017 Innovations in Power and Advanced Computing Technologies (i-PACT), Vellore, India, 21–22 April 2017; pp. 1–6.
- Karthika, M.; Nisha, K.C.R. Review on Torque Ripple Reduction Techniques of BLDC Motor. In Proceedings of the 2020 International Conference on Inventive Computation Technologies (ICICT), Coimbatore Tamilnadu, India, 26–28 February 2020; pp. 1092–1096.
- Panda, S.K.; Jian-Xin, X.; Weizhe, Q. Review of torque ripple minimization in PM synchronous motor drives. In Proceedings of the 2008 IEEE Power and Energy Society General Meeting—Conversion and Delivery of Electrical Energy in the 21st Century, Pittsburgh, PA, USA, 20–24 July 2008; pp. 1–6.
- Salah, W.A.; Ishak, D.; Hammadi, K.J. Minimization of torque ripples in BLDC motors due to phase commutation—A review. *Prz. Elektrotechniczny* **2011**, *87*, 182–188.
- Du, Z.S.; Lipo, T.A. High Torque Density and Low Torque Ripple Shaped-Magnet Machines Using Sinusoidal Plus Third Harmonic Shaped Magnets. *IEEE Trans. Ind. Appl.* **2019**, *55*, 2601–2610. [\[CrossRef\]](#)
- Yu, H.; Yu, B.; Yu, J.; Lin, C. A Dual Notched Design of Radial-Flux Permanent Magnet Motors with Low Cogging Torque and Rare Earth Material. *IEEE Trans. Magn.* **2014**, *50*, 2329139. [\[CrossRef\]](#)
- Kano, Y. Torque Ripple Reduction of Saliency-Based Sensorless Drive Concentrated-Winding IPMSM Using Novel Flux Barrier. *IEEE Trans. Ind. Appl.* **2015**, *51*, 2905–2916. [\[CrossRef\]](#)
- Li, J.; Wang, K.; Li, F. Reduction of Torque Ripple in Consequent-Pole Permanent Magnet Machines Using Staggered Rotor. *IEEE Trans. Energy Convers.* **2019**, *34*, 643–651. [\[CrossRef\]](#)
- Cho, S.; Lee, D.-C.; Hwang, J.; Kim, K.; Jang, G.U.; Bae, D.-S.; Mok, H.S.; Kim, C.-W. Optimal design to reduce torque ripple of IPM motor with radial based function meta-model considering design sensitivity analysis. *J. Mech. Sci. Technol.* **2019**, *33*, 3955–3961. [\[CrossRef\]](#)

17. Chou, P.-H.; Yang, S.-C.; Jhong, C.-J.; Huang, J.-I.; Chen, J.-Y. Permanent Magnet Motor Design for Satellite Attitude Control with High Torque Density and Low Torque Ripple. *IEEE Access* **2020**, *8*, 48587–48598. [[CrossRef](#)]
18. Jinshun, H.; Shuangfu, S.; Yiyong, Y.; Yang, W.; Wenjie, W.; Chen, X. Optimization of Torque Ripples in an Interior Permanent Magnet Synchronous Motor Based on the Orthogonal Experimental Method and MIGA and RBF Neural Networks. *IEEE Access* **2020**, *8*, 27202–27209. [[CrossRef](#)]
19. Jung, Y.-H.; Park, M.-R.; Lim, M.-S. Asymmetric Rotor Design of IPMSM for Vibration Reduction under Certain Load Condition. *IEEE Trans. Energy Convers.* **2020**, *35*, 928–937. [[CrossRef](#)]
20. Liu, H.-C.; Kim, H.; Jang, H.; Jang, I.-S.; Lee, J. Ferrite PM Optimization of SPM BLDC Motor for Oil-Pump Applications According to Magnetization Direction. *IEEE Trans. Appl. Supercond.* **2020**, *30*, 2977615. [[CrossRef](#)]
21. Liu, K.; Yin, M.; Hua, W.; Ma, Z.; Lin, M.; Kong, Y. Design and Analysis of Halbach Ironless Flywheel BLDC Motor/Generators. *IEEE Trans. Magn.* **2018**, *54*, 2833958. [[CrossRef](#)]
22. Shi, Z.; Sun, X.; Cai, Y.; Xiang, T.; Chen, L. Design optimisation of an outer-rotor permanent magnet synchronous hub motor for a low-speed campus patrol EV. *IET Electr. Power Appl.* **2020**, *14*, 2111–2118. [[CrossRef](#)]
23. Wang, S.; Hong, J.; Sun, Y.; Cao, H. Effect Comparison of Zigzag Skew PM Pole and Straight Skew Slot for Vibration Mitigation of PM Brush DC Motors. *IEEE Trans. Ind. Electron.* **2020**, *67*, 4752–4761. [[CrossRef](#)]
24. Xue, Z.-Q.; Li, H.-S.; Zhou, Y.; Ren, N.-N.; Wen, W. Analytical Prediction and Optimization of Cogging Torque in Surface-Mounted Permanent Magnet Machines with Modified Particle Swarm Optimization. *IEEE Trans. Ind. Electron.* **2017**, *64*, 9795–9805. [[CrossRef](#)]
25. Zhao, W.; Lipo, T.A.; Kwon, B.-i. Material-Efficient Permanent-Magnet Shape for Torque Pulsation Minimization in SPM Motors for Automotive Applications. *IEEE Trans. Ind. Electron.* **2014**, *61*, 5779–5787. [[CrossRef](#)]
26. Shah, S.Q.A.; Lipo, T.A.; Kwon, B.-i. Modeling of Novel Permanent Magnet Pole Shape SPM Motor for Reducing Torque Pulsation. *IEEE Trans. Magn.* **2012**, *48*, 4626–4629. [[CrossRef](#)]
27. Chen, Q.; Xu, G.; Liu, G.; Zhai, F.; Eduku, S. Reduction of Torque Ripple Caused by Slot Harmonics in FSCW Spoke-Type FPM Motors by Assisted Poles. *IEEE Trans. Ind. Electron.* **2020**, *67*, 9613–9622. [[CrossRef](#)]
28. Chen, Q.; Xu, G.; Liu, G.; Zhao, W.; Liu, L.; Zhipeng, L. Torque Ripple Reduction in Five-Phase IPM Motors by Lowering Interactional MMF. *IEEE Trans. Ind. Electron.* **2018**, *65*, 8520–8531. [[CrossRef](#)]
29. Chen, W.; Ma, J.; Wu, G.-c.; Fang, Y. Torque Ripple Reduction of a Salient-Pole Permanent Magnet Synchronous Machine with an Advanced Step-Skewed Rotor Design. *IEEE Access* **2020**, *8*, 118989–118999. [[CrossRef](#)]
30. Du, Z.S.; Lipo, T.A. Efficient Utilization of Rare Earth Permanent-Magnet Materials and Torque Ripple Reduction in Interior Permanent-Magnet Machines. *IEEE Trans. Ind. Appl.* **2017**, *53*, 3485–3495. [[CrossRef](#)]
31. Gan, C.; Wu, J.; Shen, M.; Kong, W.; Hu, Y.; Cao, W. Investigation of Short Permanent Magnet and Stator Flux Bridge Effects on Cogging Torque Mitigation in FSPM Machines. *IEEE Trans. Energy Convers.* **2018**, *33*, 845–855. [[CrossRef](#)]
32. Liu, G.; Du, X.; Zhao, W.; Chen, Q. Reduction of Torque Ripple in Inset Permanent Magnet Synchronous Motor by Magnets Shifting. *IEEE Trans. Magn.* **2017**, *53*, 2620422. [[CrossRef](#)]
33. Gandzha, S.; Sogrin, A.I.; Kiessh, I.E. The Comparative Analysis of Permanent Magnet Electric Machines with Integer and Fractional Number of Slots per Pole and Phase. *Procedia Eng.* **2015**, *129*, 408–414. [[CrossRef](#)]
34. Goss, J.; Staton, D.; Wrobel, R.; Mellor, P. Brushless AC interior-permanent magnet motor design: Comparison of slot/pole combinations and distributed vs. concentrated windings. In Proceedings of the 2013 IEEE Energy Conversion Congress and Exposition, Denver, CO, USA, 15–19 September 2013; pp. 1213–1219.
35. Li, G.-J.; Ren, B.; Zhu, Z.-Q.; Li, Y.; Ma, J. Cogging Torque Mitigation of Modular Permanent Magnet Machines. *IEEE Trans. Magn.* **2016**, *52*, 2477489. [[CrossRef](#)]
36. Su, P.; Hua, W.; Hu, M.; Wu, Z.; Si, J.; Chen, Z.; Cheng, M. Analysis of Stator Slots and Rotor Pole Pairs Combinations of Rotor-Permanent Magnet Flux-Switching Machines. *IEEE Trans. Ind. Electron.* **2020**, *67*, 906–918. [[CrossRef](#)]
37. Wu, L.; Ming, G.; Zhang, L.; Fang, Y. Improved Stator/Rotor-Pole Number Combinations for Torque Ripple Reduction in Doubly Salient PM Machines. *IEEE Trans. Ind. Electron.* **2020**, *68*, 10601–10611. [[CrossRef](#)]
38. Zhu, X.; Hua, W.; Wu, Z.; Huang, W.; Zhang, H.; Cheng, M. Analytical Approach for Cogging Torque Reduction in Flux-Switching Permanent Magnet Machines Based on Magnetomotive Force-Permeance Model. *IEEE Trans. Ind. Electron.* **2018**, *65*, 1965–1979. [[CrossRef](#)]
39. Zheng, P.; Sui, Y.; Zhao, J.; Tong, C.; Lipo, T.A.; Wang, A. Investigation of a Novel Five-Phase Modular Permanent-Magnet In-Wheel Motor. *IEEE Trans. Magn.* **2011**, *47*, 4084–4087. [[CrossRef](#)]
40. Sung, S.; Jang, G.; Kang, K. Noise and vibration due to rotor eccentricity in a HDD spindle system. *Microsyst. Technol.* **2014**, *20*, 1461–1469. [[CrossRef](#)]
41. Nizam, M.; Tri Waloyo, H.; Inayati, I. Brushless Direct Current Electric Motor Design with Minimum Cogging Torque. In Proceedings of the International Conference on Electrical Engineering, Computer Science and Informatics (EECSI 2014), Yogyakarta, Indonesia, 20–21 August 2014; p. 342. [[CrossRef](#)]
42. Kim, K.-S.; Lee, C.-M.; Hwang, G.-Y.; Hwang, S.-M. Effect of the number of poles on the acoustic noise from BLDC motors. *J. Mech. Sci. Technol.* **2011**, *25*, 273–277. [[CrossRef](#)]
43. Fei, W.; Shen, J.-X.; Wang, C.; Luk, P.C.-K. Design and analysis of a new outer-rotor permanent-magnet flux-switching machine for electric vehicle propulsion. *COMPEL Int. J. Comput. Math. Electr. Electron. Eng.* **2011**, *30*, 48–61. [[CrossRef](#)]

44. Zhu, Z.-Q. Fractional slot permanent magnet brushless machines and drives for electric and hybrid propulsion systems. *COMPEL Int. J. Comput. Math. Electr. Electron. Eng.* **2011**, *30*, 9–31. [[CrossRef](#)]
45. Li, Y.; Zhu, Z.-Q.; Wu, X.; Thomas, A.; Zhan-Yuan, W. Comparative Study of Modular Dual 3-Phase Permanent Magnet Machines with Overlapping/Non-overlapping Windings. *IEEE Trans. Ind. Appl.* **2019**, *55*, 3566–3576. [[CrossRef](#)]
46. Ou, L.; Wang, X.; Xiong, F.; Ye, C. Reduction of torque ripple in a wound-rotor brushless doubly-fed machine by using the tooth notching. *IET Electr. Power Appl.* **2018**, *12*, 635–642. [[CrossRef](#)]
47. Sculler, F.; Becker, F.; Zahr, H.; Semail, E. Design of a Bi-Harmonic 7-Phase PM Machine with Tooth-Concentrated Winding. *IEEE Trans. Energy Convers.* **2020**, *35*, 1567–1576. [[CrossRef](#)]
48. Sun, H.Y.; Wang, K.; Liu, L.; Zhu, S.; Liu, C. EMF Voltage Distortion Mitigation in Fractional-Slot Permanent Magnet Machines by Varying Coil Distribution and Turn Ratio. *IEEE Trans. Magn.* **2021**, *57*, 3027020. [[CrossRef](#)]
49. Zhiqing, Z.; Yong-bin, C. Design and Analysis of a Novel Two Phase Doubly Salient Permanent Magnet Machine. *TELKOMNIKA Indones. J. Electr. Eng.* **2014**, *12*, 234–244. [[CrossRef](#)]
50. Ahsanullah, K.; Dutta, R.; Rahman, M.F. Preliminary Design Analysis of Low Speed Interior Permanent Magnet Machine with Distributed and Concentrated Windings. *J. Int. Conf. Electr. Mach. Syst.* **2014**, *3*, 139–147. [[CrossRef](#)]
51. Xiaogang, L.; Dinyu, Q.; Lipo, T.A. A novel two phase doubly salient permanent magnet motor. In Proceedings of the IAS '96. Conference Record of the 1996 IEEE Industry Applications Conference Thirty-First IAS Annual Meeting, San Diego, CA, USA, 6–10 October 1996; Volume 802, pp. 808–815.
52. Surong, H.; Aydin, M.; Lipo, T.A. Torque quality assessment and sizing optimization for surface mounted permanent magnet machines. In Proceedings of the Conference Record of the 2001 IEEE Industry Applications Conference, 36th IAS Annual Meeting (Cat. No.01CH37248), Chicago, IL, USA, 30 September–4 October 2001; pp. 1603–1610.
53. Huang, S.; Aydin, M.; Lipo, T.A. Electromagnetic vibration and noise assessment for surface mounted PM machines. In Proceedings of the 2001 Power Engineering Society Summer Meeting, Conference Proceedings (Cat. No.01CH37262), Vancouver, BC, Canada, 15–19 July 2001; pp. 1417–1426.
54. Bouloukza, I.; Mordjaoui, M.; Kurt, E.; Bal, G.; Ökmen, C. Electromagnetic design of a new radial flux permanent magnet motor. *J. Energy Syst.* **2018**, *2*, 13–27. [[CrossRef](#)]
55. Koo, B.; Kim, J.; Nam, K. Halbach Array PM Machine Design for High Speed Dynamo Motor. *IEEE Trans. Magn.* **2021**, *57*, 3022894. [[CrossRef](#)]
56. Momen, F.; Rahman, K.M.; Son, Y. Electrical Propulsion System Design of Chevrolet Bolt Battery Electric Vehicle. *IEEE Trans. Ind. Appl.* **2019**, *55*, 376–384. [[CrossRef](#)]
57. Neethu, S.; Nikam, S.P.; Pal, S.; Wankhede, A.K.; Fernandes, B.G. Performance Comparison Between PCB-Stator and Laminated-Core-Stator-Based Designs of Axial Flux Permanent Magnet Motors for High-Speed Low-Power Applications. *IEEE Trans. Ind. Electron.* **2020**, *67*, 5269–5277. [[CrossRef](#)]
58. Petrov, I.; Ponomarev, P.; Alexandrova, Y.; Pyrhonen, J. Unequal Teeth Widths for Torque Ripple Reduction in Permanent Magnet Synchronous Machines with Fractional-Slot Non-Overlapping Windings. *IEEE Trans. Magn.* **2015**, *51*, 2355178. [[CrossRef](#)]
59. Shi, Z.; Sun, X.; Lei, G.; Yang, Z.; Guo, Y.; Zhu, J. Analysis and Optimization of Radial Force of Permanent-Magnet Synchronous Hub Motors. *IEEE Trans. Magn.* **2020**, *56*, 2953731. [[CrossRef](#)]
60. Ueda, Y.; Takahashi, H. Transverse-Flux Motor Design with Skewed and Unequally Distributed Armature Cores for Reducing Cogging Torque. *IEEE Trans. Magn.* **2017**, *53*, 2703087. [[CrossRef](#)]
61. Yang, Y.; Castano, S.M.; Yang, R.; Kasprzak, M.; Bilgin, B.; Sathyan, A.; Dadkhah, H.; Emadi, A. Design and Comparison of Interior Permanent Magnet Motor Topologies for Traction Applications. *IEEE Trans. Transp. Electrification.* **2017**, *3*, 86–97. [[CrossRef](#)]
62. Yeşilbağ, E.; Ertuğrul, Y.; Ergene, L.T. Axial flux PM BLDC motor design methodology and comparison with a radial flux PM BLDC motor. *Turk. J. Electr. Eng. Comput. Sci.* **2017**, *25*, 3455–3467. [[CrossRef](#)]
63. Baig, M.A.; Ikram, J.; Iftikhar, A.; Bukhari, S.S.H.; Khan, N.; Ro, J.-S. Minimization of Cogging Torque in Axial Field Flux Switching Machine Using Arc Shaped Triangular Magnets. *IEEE Access* **2020**, *8*, 227193–227201. [[CrossRef](#)]
64. Du, Z.S.; Lipo, T.A. Reducing Torque Ripple Using Axial Pole Shaping in Interior Permanent Magnet Machines. *IEEE Trans. Ind. Appl.* **2020**, *56*, 148–157. [[CrossRef](#)]
65. Hu, Y.; Zhu, S.; Liu, C.; Wang, K. Electromagnetic Performance Analysis of Interior PM Machines for Electric Vehicle Applications. *IEEE Trans. Energy Convers.* **2018**, *33*, 199–208. [[CrossRef](#)]
66. Jung, Y.-H.; Lim, M.-S.; Yoon, M.-H.; Jeong, J.-S.; Hong, J.-P. Torque Ripple Reduction of IPMSM Applying Asymmetric Rotor Shape under Certain Load Condition. *IEEE Trans. Energy Convers.* **2018**, *33*, 333–340. [[CrossRef](#)]
67. Li, B.; Zhao, J.; Mou, Q.; Liu, X.; Haddad, A.; Liang, J. Research on torque characteristics of a modular arc-linear flux switching permanent-magnet motor. *IEEE Access* **2019**, *7*, 57312–57320. [[CrossRef](#)]
68. Song, C.-H.; Kim, H.; Kim, K.-C. Design of a Novel IPMSM Bridge for Torque Ripple Reduction. *IEEE Trans. Magn.* **2021**, *57*, 3016985. [[CrossRef](#)]
69. Torkaman, H.; Ghaheri, A.; Keyhani, A. Design of Rotor Excited Axial Flux-Switching Permanent Magnet Machine. *IEEE Trans. Energy Convers.* **2018**, *33*, 1175–1183. [[CrossRef](#)]
70. Wang, K.; Liang, Y.; Wang, D.; Wang, C. Cogging torque reduction by eccentric structure of teeth in external rotor permanent magnet synchronous motors. *IET Electr. Power Appl.* **2018**, *13*, 57–63. [[CrossRef](#)]

71. Wu, R.; Xu, Q.; Qiong, L.; Zhou, L. Reduction of Cogging Torque and Torque Ripple in Interior PM Machines With Asymmetrical V-Type Rotor Design. *IEEE Trans. Magn.* **2016**, *52*, 2530840. [[CrossRef](#)]
72. Yousuf, M.; Khan, F.; Ikram, J.; Badar, R.; Bukhari, S.S.H.; Ro, J.-S. Reduction of Torque Ripples in Multi-Stack Slotless Axial Flux Machine by Using Right Angled Trapezoidal Permanent Magnet. *IEEE Access* **2021**, *9*, 22760–22773. [[CrossRef](#)]
73. Zhu, X.; Hua, W. An Improved Configuration for Cogging Torque Reduction in Flux-Reversal Permanent Magnet Machines. *IEEE Trans. Magn.* **2017**, *53*, 2655727. [[CrossRef](#)]
74. Zhu, X.; Hua, W.; Wu, Z. Cogging torque minimisation in FSPM machines by right-angle-based tooth chamfering technique. *IET Electr. Power Appl.* **2018**, *12*, 627–634. [[CrossRef](#)]
75. Toba, A.; Lipo, T.A. Generic torque-maximizing design methodology of surface permanent-magnet vernier machine. *IEEE Trans. Ind. Appl.* **2000**, *36*, 1539–1546. [[CrossRef](#)]
76. Zhao, J.; Yan, Y.; Li, B.; Liu, X.; Zhen, C. Influence of Different Rotor Teeth Shapes on the Performance of Flux Switching Permanent Magnet Machines Used for Electric Vehicles. *Energies* **2014**, *7*, 8056–8075. [[CrossRef](#)]
77. Wei, S.; Zhouyun, Z. Multiobjective optimum design method with anti-demagnetization of high-density permanent magnet synchronous motor. *IEEJ Trans. Electr. Electron. Eng.* **2014**, *9*, 555–562. [[CrossRef](#)]
78. Shin, P.S.; Kim, H.Y.; Kim, Y.B. Minimization of Torque Ripple for an IPMSM with a Notched Rotor Using the Particle Swarm Optimization Method. *J. Electr. Eng. Technol.* **2014**, *9*, 1577–1581. [[CrossRef](#)]
79. Shen, J.-X.; Shi, D.; Wang, C.; Li, P.; Wang, K.; Jin, M.-J. Torque ripple analysis for IPM AC motors. *COMPEL Int. J. Comput. Math. Electr. Electron. Eng.* **2014**, *33*, 1514–1526. [[CrossRef](#)]
80. Lee, C.-U.; Kim, D.; Kim, D.-H. Robust Design Optimization for Reducing Cogging Torque of a BLDC Motor through an Enhanced Taguchi Method. *J. Korean Magn. Soc.* **2014**, *24*, 160–164. [[CrossRef](#)]
81. Kim, K.-C. Study of the Reduction of Torque Ripples for Multi-pole Interior Permanent Magnet Synchronous Motors using Rotor Saliency. *J. Korea Acad. Ind. Coop. Soc.* **2014**, *15*, 6270–6275. [[CrossRef](#)]
82. Kim, J.-H.; Seo, J.-M.; Jung, H.-K.; Won, C.-Y. Analysis and Design of a Novel-Shape Permanent Magnet Synchronous Motor for Minimization of Torque Ripple and Iron Loss. *J. Magn.* **2014**, *19*, 411–417. [[CrossRef](#)]
83. Cvetkovski, G.; Petkovska, L. Cogging torque minimisation of PM synchronous motor using genetic algorithm. *Int. J. Appl. Electromagn. Mech.* **2014**, *46*, 327–334. [[CrossRef](#)]
84. Cui, J.; Xiao, W.; Longhua, W.; Hao, F.; Jianbo, Z.; Wang, H. Optimization design of low-speed surface-mounted PMSM for pumping unit. *Int. J. Appl. Electromagn. Mech.* **2014**, *46*, 217–228. [[CrossRef](#)]
85. Soleimani, J.; Vahedi, A.; Mirimani, S.M. Inner Permanent Magnet Synchronous Machine Optimization for HEV Traction Drive Application in Order to Achieve Maximum Torque per Ampere. *Iran. J. Electr. Electron. Eng.* **2011**, *7*, 241–248.
86. Rashidaee, S.; Gholamian, S.A. Reduction of cogging torque in ipm motors by using the taguchi and finite element method. *Int. J. Comput. Sci. Eng. Surv.* **2011**, *2*, 1–10. [[CrossRef](#)]
87. Meng, X.; Wang, S.; Qiu, J.; Zhu, J.; Guo, Y. Cogging torque reduction of Bldc motor using level set based topology optimization incorporating with triangular finite element. *Int. J. Appl. Electromagn. Mech.* **2010**, *33*, 1069–1076. [[CrossRef](#)]
88. Masmoudi, A. On the sizing of fractional slot PM machines oriented towards the improvement of their torque production capability. *COMPEL Int. J. Comput. Math. Electr. Electron. Eng.* **2011**, *30*, 32–47. [[CrossRef](#)]
89. Lim, S.-B.; Park, H.-J.; Kang, D.-W.; Ham, S.-H.; Lee, J. Surface Mounted Permanent Magnet Synchronous Motor Design for Torque Ripple Reduction in EPS. *J. Korean Inst. Illum. Electr. Install. Eng.* **2010**, *24*, 27–31. [[CrossRef](#)]
90. Lee, J.H.; Lee, T.H. Optimum Design Criteria for Maximum Torque Density and Minimum Torque Ripple of Flux Switching Motor using Response Surface Methodology. *J. Magn.* **2010**, *15*, 74–77. [[CrossRef](#)]
91. Kang, D.-W.; Go, S.-C.; Won, S.H.; Lim, S.-B.; Lee, J. Analysis of the Torque Characteristics of a Multi-Degrees of Freedom Surface Permanent-Magnet Motor. *J. Magn.* **2010**, *15*, 36–39. [[CrossRef](#)]
92. Hwang, C.-C.; Chang, C.-M.; Li, P.-L.; Liu, C.T. Design of rotor shape to reduce torque ripple in IPM motors. *J. Phys. Conf. Ser.* **2011**, *266*, 012068. [[CrossRef](#)]
93. Hur, J.; Kim, B.-W. Rotor Shape Design of an Interior PM Type BLDC Motor for Improving Mechanical Vibration and EMI Characteristics. *J. Electr. Eng. Technol.* **2010**, *5*, 462–467. [[CrossRef](#)]
94. Hongliang, Y.; Zhang, Z.; Gong, J.; Huang, S.; Ding, X. Application for Step-skewing of Rotor of IPM Motors Used in EV. *World Electr. Veh. J.* **2010**, *4*, 532–536. [[CrossRef](#)]
95. Hafner, M.; Franck, D.; Hameyer, K. Accounting for saturation in conformal mapping modeling of a permanent magnet synchronous machine. *COMPEL Int. J. Comput. Math. Electr. Electron. Eng.* **2011**, *30*, 916–928. [[CrossRef](#)]
96. Choi, G.-S.; Hahn, S.-C. Multiobjective Optimal Double-Layer PM Rotor Structure Design of IPMSM by Response Surface Method and Finite Element Method. *J. Korean Inst. Illum. Electr. Install. Eng.* **2010**, *24*, 123–130. [[CrossRef](#)]